Since January 2020 Elsevier has created a COVID-19 resource centre with free information in English and Mandarin on the novel coronavirus COVID-19. The COVID-19 resource centre is hosted on Elsevier Connect, the company's public news and information website.

Spectrochimica Acta Part A: Molecular and Biomolecular Spectroscopy 244 (2021) 118837

Contents lists available at ScienceDirect

Spectrochimica Acta Part A: Molecular and Biomolecular Spectroscopy

journal homepage: www.elsevier.com/locate/saa

Evaluation of nutrition components in Lanzhou lily bulb by confocal Raman microscopy

Yuee Li *, Huihui Wang, Wenbo Zhang, Haining Wu, Zhong Wang

School of Information Science and Engineering, Lanzhou University, Lanzhou, Gansu 730000, China

ARTICLE INFO

Article history:
Received 27 May 2020
Received in revised form 24 July 2020
Accepted 12 August 2020
Available online 17 August 2020

Keywords:
Lanzhou lily
Raman spectrum
Nutrition content
Starch

ABSTRACT

Lanzhou lily is a famous lily variety in China, which has many advantages different from other lily varieties. It is rich in nutrients and can be used as medicine or food. The present study is performed to evaluate the quality of Lanzhou lily by Raman spectroscopy. Here, Raman spectra of lily bulbs were collected by confocal Raman microscopy. Through study of a variety of samples, we found that Raman peaks of several important nutrients including starch, sucrose and amino acids were clearly observed from scales of lily bulb, while strong characteristic peaks of ferulic acid were observed at the epidermis of the same scale due to the stimulation of the external environment. We also compared lily bulbs with various sizes and shapes using an average Raman spectrum of selected area. Then, changes of nutrients were quantitively analyzed in different storage period. The results show that the nutrient components including starch, sucrose, amino acids and ferulic acid can be evaluated by Raman spectroscopy. Then the quality of Lanzhou lily can be evaluated by Raman spectroscopy. This is valuable for quality evaluation of lily using non-destructive methods.

1. Introduction

Lily is a perennial herbaceous bulbous plant of the Lilium in the liliaceae family [1], which is native to China. It has been recorded in *Shen Nong's herbal classic* (one of the four great works of Traditional Chinese medicine of Han nationality, the earliest extant works of traditional Chinese medicine) since 1st century BCE. The lily, in this case, is the subterranean modification of stem, which is made up of numerous hypertrophic scales. There are multitudinous lilies in China, among which the hybrid lines of Asiatic lily are Lilium pumilum, *Lilium lancifolium* and Lilium davidii Duchartre. Lanzhou lily studied here is a famous variety of Lilium davidii Duchartre.

Lanzhou in Gansu province has a semi-arid climate, high altitude and large temperature difference between day and night, which create a proper condition for the accumulation of sugars in plants, so the only sweet lily variety that can be used for both medicine and food has been cultivated and developed here. It has been approved as geographical indications protection products, by the General Administration of Quality Supervision, Inspection and Quarantine of the People's Republic of China. In addition, lilies have lung-clearing properties [2], and Euijeong Lee et al. found in their study that lily has a protective effect on pneumonia caused by cigarette smoke [3], making it possible to help patients infected with COVID-19.

Currently, chemical analyses are broadly used for the evaluation of biochemical components, including gas chromatography, high-performance liquid chromatography, and gas chromatography mass spectrometry [4]. These destructive methods are time consuming and professional technicians are needed for handling of special protocols and instruments [5]. In addition, it is difficult to obtain the spatial distribution of a specific substance in a sample.

Raman spectroscopy has attracted extensive attention in biological field for analyzing cells or various biological tissues in recent years. Raman spectroscopy is an optical technique based on inelastic scattering of light of vibrating molecules. Biomolecules with diverse functional groups exhibit different characteristic peaks in Raman spectrum due to different vibration modes, so Raman spectrum can provide chemical fingerprints of cells, tissues or biofluids. Notably, compared with infrared spectrum, which is also derived from molecular vibration modes, the measurement of Raman spectroscopy is not influenced by the existence of water. This provides great convenience for sample detection, particularly for water-rich samples [6]. Moreover, no special sample preparations are required and it is possible to achieve nondestructive testing. Furthermore, Raman imaging can also be performed to obtain the distribution of some components of interest. It is important to study the distribution of one specific component in many fields such as pharmacy, medicine, and biology etc. Monika Szyman'ska-Chargot et al. [7] observed the distribution variation of polysaccharides in the cell wall during the development and aging of apple fruits using Raman imaging. Christoph Krafft et al. [8] performed Raman microscopic imaging for different functional groups and presented the distribution of amygdalin in

* Corresponding author.
E-mail address: liyuee@lzu.edu.cn (Y. Li).

https://doi.org/10.1016/j.saa.2020.118837
1386-1425/

apricot seeds. In a recent study, tiny residual tumors on the surface of breast excision specimens within surgical timescales were identified by Raman spectroscopy combination with other techniques, which permits for accurate remove of tumor tissue [9]. Furong Tian et al. [10] proposed a novel strategy based on plasma-tunable Raman/FTIR imaging to track the delivery and release of an anticancer drug (Mitoxantrone-MTX) by gold nanostars.

The evaluation method and standard for Lanzhou lily has not been established. Lilies with larger size are generally considered to have better quality, so it is sold at a higher price. In this work, we investigated the nutritional ingredients in Lanzhou lily bulb using Raman spectroscopy. It provides a way for quantitively evaluating the quality of lilies nondestructively.

2. Materials and experiments

2.1. Preparation of sample

It takes a long time to plant Lanzhou lily, seeds shall be made from seed pellets cultivated in the seed cropland. After growing in the field for 3 years, the lilies should be dug up and cultivated in the other cropland for 3 years, then some of these lilies would be replanted again. Hence Lanzhou lilies of high quality sold in the market are usually grown for more than 6 years. Nevertheless, after many years of cultivation, the senescent scales may cause the bulbs to divide and a tightly packed lily split into several loose bulbs, reducing the quality of lily.

Lilies are usually planted in October and harvested in the late October or the early spring. Fresh Lanzhou lilies are dug up from one of the biggest plantation bases (Guanshan Township, Yongjing County, Linxia Autonomous Prefecture, Gansu Province, China) in the late September 2019 (abnormal harvesting time, referred to as "the first batch" below) and in the late October 2019 (mass harvesting time, referred to as "the second batch" below). Typical samples were selected from each batch according to the appearance of lily (size and whether divided) for experiments (Fig. 1).

Lanzhou lilies are usually stored in refrigeration house after they have been picked, then these lilies in the same batch are generally classified into different quality grades, according to their appearances (size and whether divided). Here, we kept all samples in the refrigerator of the laboratory (at about 5 °C and was kept a certain humidity). 9 lilies from each batch were selected as measurement samples covering all kinds of sizes (classified by diameter and mass) and segmented lilies, among which the lily with the smallest diameter could only be used as a seed. To conduct the comparison of lilies with consistency, all inner scales are taken from the center of the lily and all outer scales are taken from the outermost second layer. The Raman spectra of each sample were collected at day 0, 15 and 30.

2.2. Measurement of Raman spectra

All Raman spectra were acquired using the Alpha confocal Raman microscope system (WiTec, Germany) equipped with 532 nm (Verdi v-6) laser excitation, and ACTON 300i spectrometer with Pixis Spec 10–100× CCD camera (Princeton Instruments, Trenton, NJ) for Raman signal detection. The laser beam was focused into the sample by a Zeiss LD EC Epiplan-Neofluar 10× and 50× objective lens with NA 0.55 (Nikon, Japan). We set the laser power at 10 mW for Raman measurement to ensure a high SNR and not damage the lily tissue. The integration time is 5 s per pixel. The laser spot entered the sample at the same depth and the average spectrum of randomly selected multiple points of samples are used for comparison of different samples.

WiTec Project 5.0 was used for removal of cosmic rays, baseline correction, smoothing and denoising. Then, the pre-processed spectrum was exported for further analysis using MATLAB R2016b.

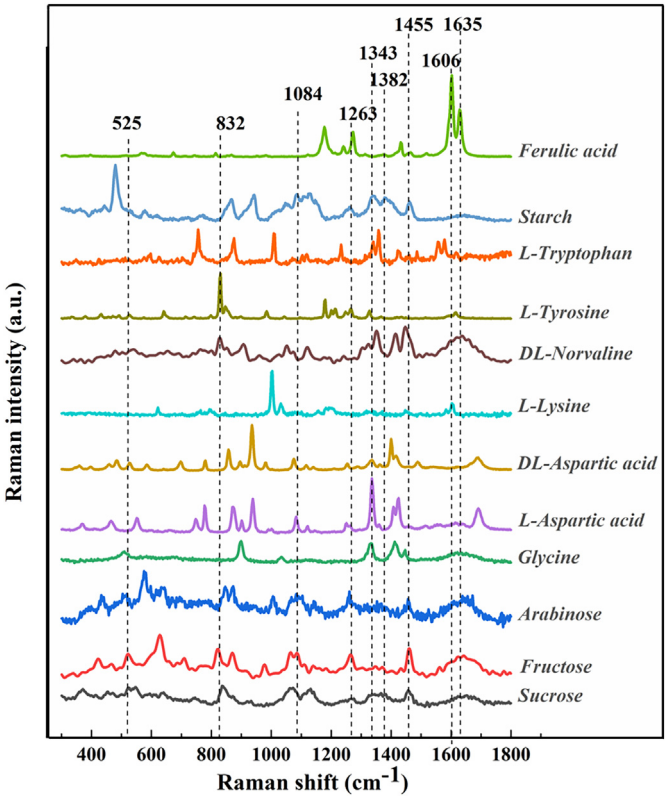

Fig. 2. Raman spectra of 12 pure substances (in the range of 300 to 1800 cm^{-1}).

3. Results and discussion

To facilitate the analysis of possible components in Lanzhou lily by Raman spectroscopy, the Raman spectra of 7 types of amino acids, 4 types of carbohydrate and ferulic acid were measured and shown in Fig. 2.

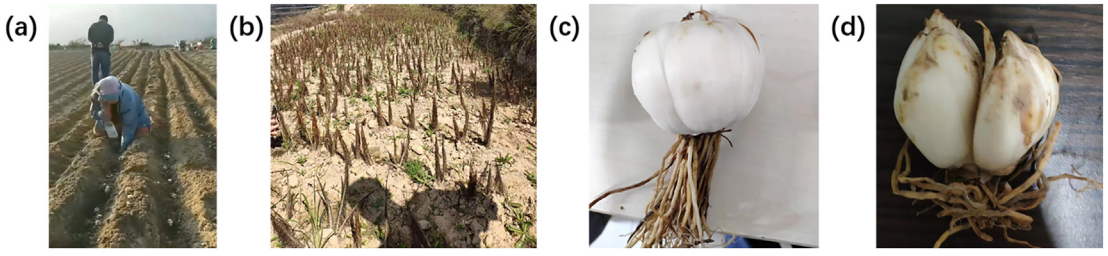

Fig. 1. Planting Lanzhou lilies and lily appearance: (a) transfer the seed balls from the seed to another field; (b) the aboveground part of Lanzhou lilies that would be dug; (c) normal Lanzhou lily; (d) divided lily.

3.1. Different positions of Lanzhou lily

Fig. 3(a, b) gives microscopic images of the epidermis and internal matrix of outer scales from Lanzhou lily. Similar to that of onion scales, the cells in the outermost epidermis (as a "membrane") owns thinner structures and neater arrangement compared with stromal cells in the internal matrix of lily. We compared the epidermis and stromal cells for outer scales by Raman spectroscopy.

The region between 300 and 2000 cm^{-1} is considered to be the fingerprint region for our analysis. The average Raman spectra of epidermis and matrix of outer scales are shown in Fig. 3(c). Abundant Raman Peaks can be observed for the matrix, including 479 cm^{-1}, 870 cm^{-1}, 942 cm^{-1}, 1084 cm^{-1}, 1263 cm^{-1}, 1343 cm^{-1}, 1382 cm^{-1} and 1457 cm^{-1}. However, the epidermis displays fewer peaks. The most prominent feature is that it contains the aromatic ring stretching vibration at 1606 cm^{-1} and the C═C stretching vibration [11,12] near 1635 cm^{-1} with high strength, indicating that ferulic acid is abundant in the scale epidermis. As shown in Fig. 2, tyrosine, lysine and ferulic acid all have peaks in this region, but ferulic acid contributes more than other components. However, it does not mean the matrix of internal scales contains ferulic acid as low as that of the outer scales. As shown in Fig. 3(d), the matrix of the inner scales contains much more ferulic acid, which is a ubiquitous floristic constituent that arises from the metabolism of phenylalanine and tyrosine. By virtue of effectively scavenging deleterious radicals and suppressing radiation-induced oxidative reactions, ferulic acid may serve as an important antioxidant in preserving physiological integrity of cells exposed to air and irradiated by UV radiation [13]. The ferulic acid is widely found in lily bulbs, and the extensive exposure of the outer scales to air and even other adverse environments triggers a stress response: ferulic acid is transferred from the matrix of the outer scales to the epidermis to form a protective film. In fact, in a previous study [14], HPLC-MS was used to determine 11 polyphenols of lily bulbs including ferulic acid, whose antioxidant capacity had been tested experimentally. It needs to be mentioned that we could not determine the presence of other polyphenols such as gallic acid and eugenic acid from Raman spectrum of lily. It was also found that 1635 cm^{-1} moves to 1640 cm^{-1}. That may mean glycine or L-histidine exhibits distribution similar to ferulic acid in different scale locations [15].

In order to distinguish the epidermis and matrix of the outer scale more intuitively, we acquired Raman spectra along a straight line (red line in Fig. 4(a)) from the epidermis to the matrix on the cut surface of the outer scale. Raman spectra of 50 points on the line were shown to display the variation of various substances along the line in Fig. 4(b). We also gave Raman spectra of 8 typical points in Fig. 4(c) (the same color is used for positional matchup). Along this line peaks of ferulic acid in the epidermis firstly rose and reached its maximum at the blue and yellow points, then went down. Because the points in the tail of the line are part of the matrix, the Raman spectrum there shows similar characteristics with that of Fig. 3(d).

3.2. Influence of storage time

According to our investigation, after digging up, Lanzhou lily would be placed in the refrigeration house for storage, and then sorted and vacuum-packed before being going to the market. The possible storage time was roughly covered in our study. We studied the variation of components during storage by using average Raman spectra, considering both internal and external scales of each bulb. In our experiments, all Raman spectra are normalized by the Raman peak of water for

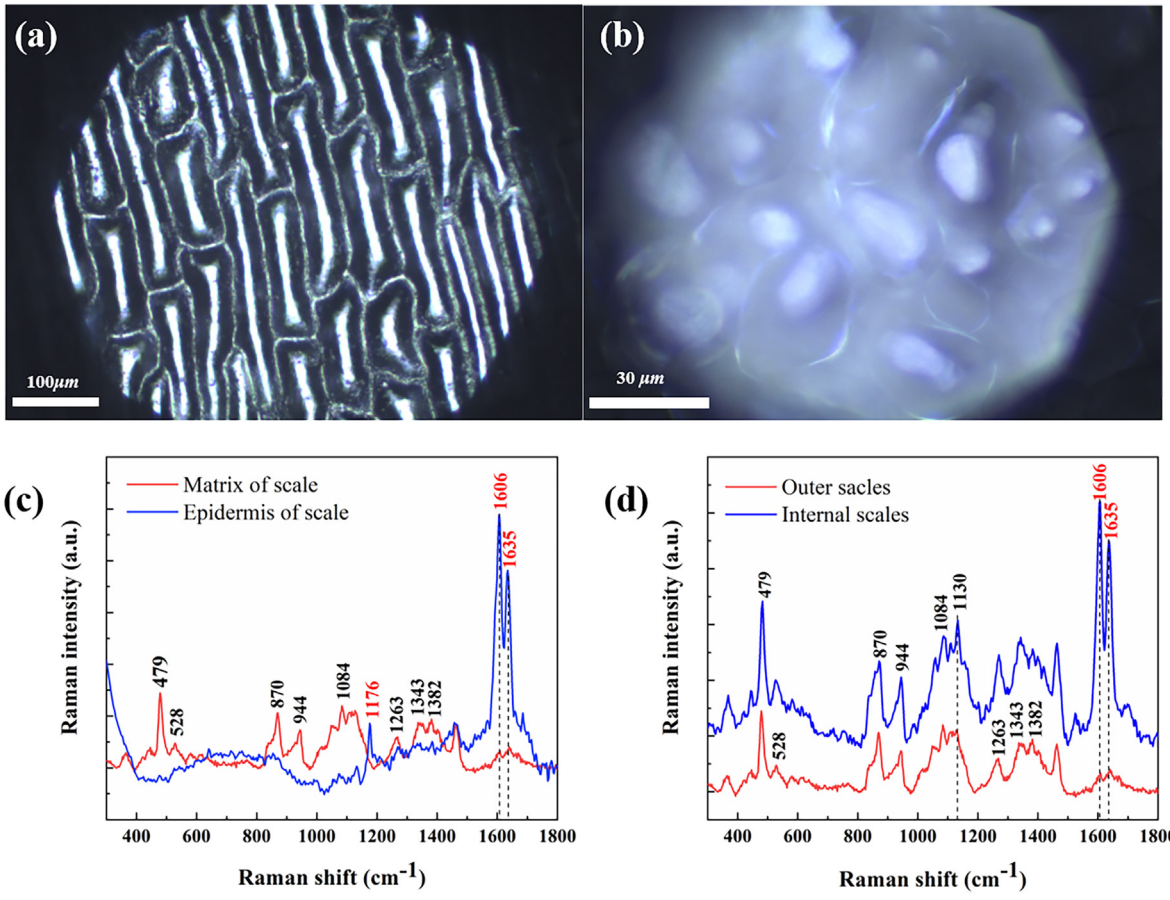

Fig. 3. Cells in lily scale: (a) epicuticular cell; (b) internal matrix cell and Raman spectrum of Lanzhou lily at different positions: (c) matrix and epidermis of outer scales; (d) matrix of internal and outer scales.

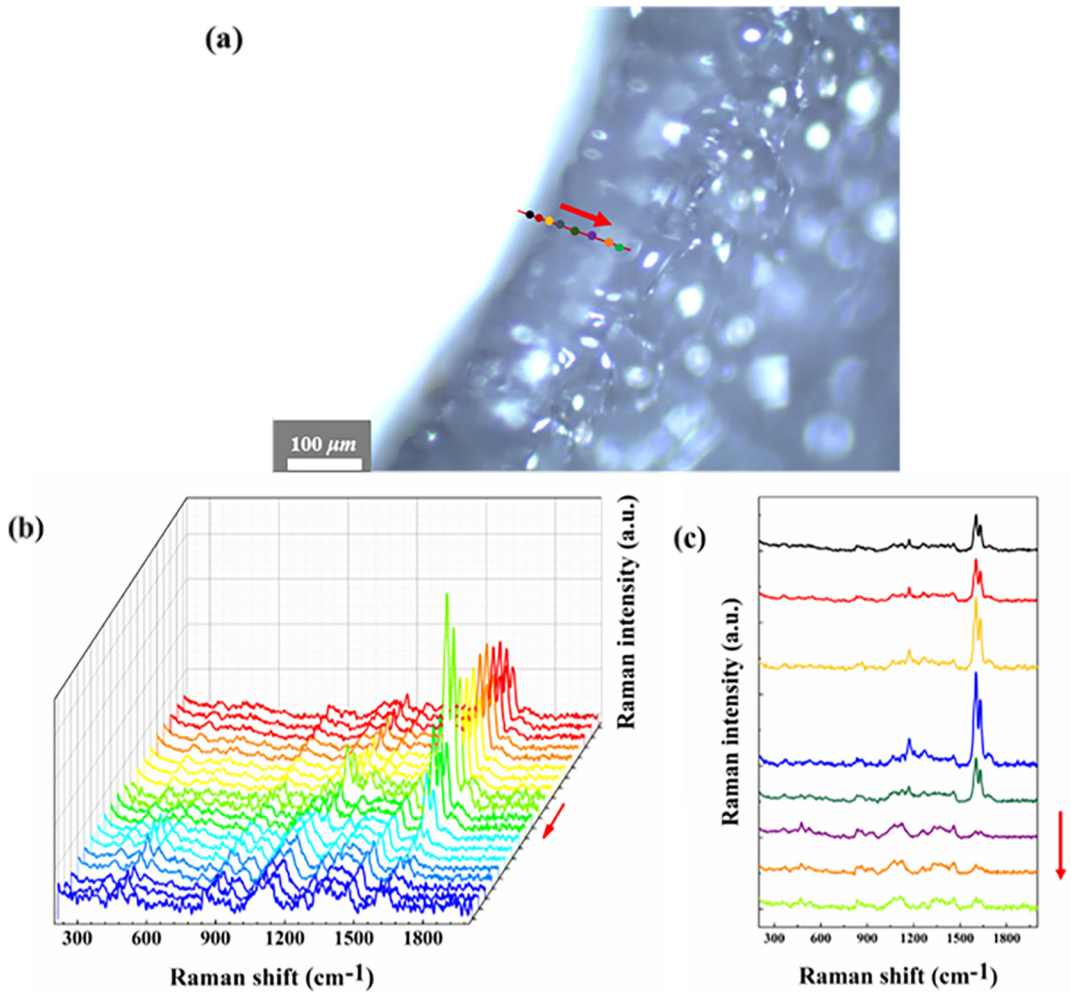

Fig. 4. (a) Microscopic image of section of lily's outer scales, Raman spectra were collected along the red line with a length of 150 μm; (b) a waterfall plot for Raman spectra on the line, in which the color has nothing to do with the color of the points; (c)Raman spectra of 8 points. The red arrows in each figure indicate the direction from the epidermis to the matrix.

comparison of these samples in different storage time. The normalization coefficient is calibrated by considering water loss. The weight of the samples is shown in Fig. 5(a). Most Lanzhou lilies in the market are harvested in October, so we chose the second batch for testing.

Respiratory consumption of carbohydrates during storage is well represented in the Raman spectrum, see Fig. 5(b-c). Typical Raman characteristic bands attributed to carbohydrate, such as 479 cm^{-1}, 870 cm^{-1}, 942 cm^{-1}, 1082 cm^{-1} and 1127 cm^{-1}, can be observed in the matrix. The bands of starch mentioned above are gradually decreasing in strength, especially in the first 15 days, which means the consumption rate decreases after 15 days. Lily is a kind of non-climacteric respiratory food. Unlike the climacteric fruit ripening, ethylene plays a key role and the regulation mechanism of this kind of fruit ripening is not clear. A single consistent pattern of hormone changes does not occur in this group of fruit during ripening [16]. For this type of plant, the respiration rate is very high at the beginning of storage, and then drops to a very low level. Similar to freshly harvested potato tubers [17], Lanzhou lilies require a period of after-ripening. Lanzhou lily has a dormancy time longer than potato, so it can be stored for months under the proper environment generally.

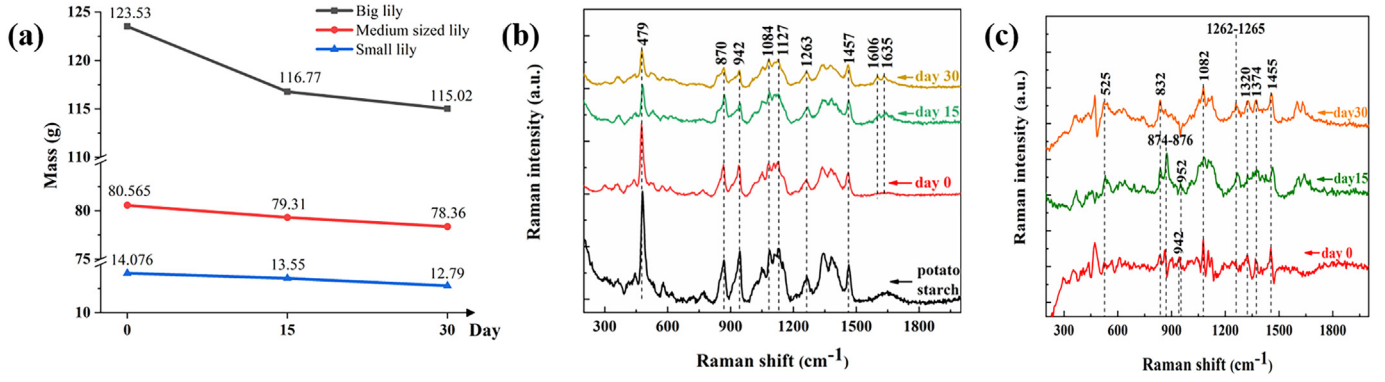

Fig. 5. (a) Mass variation trend of Lanzhou lily bulbs; (b) Raman spectrum of photo starch (analytic reagent) and Lanzhou lily; (c) Raman spectrum of Lanzhou lily after subtraction of photo starch.

Lily starch, like other starches, exists in the form of crystalline in its natural state. Natural starch is usually divided into type A, B and C according to its X-ray diffraction (XRD) characteristics. Grain starch, such as corn, wheat and rice, generally belongs to type A; while rhizome or tuber and fruit starch, such as potato, mango and banana, are usually type B; Type C may be a mixture of type A and type B starch. Lily starch belongs to type B [2]. We used Raman spectra of potato starch gel close to lily starch for quantitative analysis of starch, see Fig. 5(b).

The Raman spectrum confirms that Lanzhou lily is a food with very high starch content. Wu Lihua et al. [18] successfully isolated the amylopectin and amylopectin of lily in the 1990s. The spectra of fresh lily were almost identical to the starch spectra in particular, except for the skeletal mode at 942 cm^{-1} containing the α-(1 → 4) linkage [19]. Therefore, the Raman peaks of starch are likely to annihilate the bands of other substances. In order to eliminate the influence of it, the Raman spectrum of pure starch was subtracted from the Raman spectrum of lily by taking the peak at 479 cm^{-1} (Stretching vibration of the carbonated skeletal [20]) as the standard value. Then the resulting spectrum is used for analysis of other nutrients with lower concentration (Fig. 5(c)). The typical bands are given in Table 1. In addition to these distinct characteristic peaks, the peaks of various amino acids are also exposed in the spectra, including 832 cm^{-1}, 1082 cm^{-1} and 1455 cm^{-1}. However, due to the overlapping of characteristic bands of various amino acids, it is difficult to distinguish them. A study showed that lily bulb contains 17 amino acids, which is an ideal protein source [21]. Although carbohydrate such as sucrose is the main source of sweetness in lily bulbs, the presence of free amino acids in the scales, especially glycine, may also contribute to sweetness. Glycine has a distinctive sweet taste and serves to cover up bitterness.

As shown in Fig. 5, after 15 days storage, the Raman peaks of other components, including various amino acids, enhance compared with the fresh lily. The phospholipid band at 876 cm^{-1} shows up and abundant peaks of other diverse types of carbohydrates are observed on these spectra in Fig. 5(b), for instance, sucrose at 874 cm^{-1}, 1263 cm^{-1}, 1455 cm^{-1} and β-glucan at 1374 cm^{-1}. The 1082 cm^{-1} peak characterized by P═O vibration shows the presence of phytic acid, which is widely found in plant seeds and is a beneficial nutrient for human body. Its products are inositol and phospholipid, the former of which has anti-aging effect and the latter of which is an important part of human cells. Little change can be observed in the second 15 days. This may be related to the dormant period mentioned above, during which the invariable state of lily bulbs results in stable Raman spectra. Over a longer period, the loss of carbohydrate is relatively small compared to other similar crops.

In another study, the author conducted a chemical test on Lanzhou lily. The pretest showed that Lanzhou lily bulbs contained polysaccharides, glycosides, amino acids (polypeptides, proteins), saponins, lipids, alkaloids, etc. Subsequently, ^{1}H NMR, ^{13}C NMR, DEPT and MS were used to analyze the separated and purified components from lily.

Table 1
Assignment of peaks in Raman spectra.

Band position (cm^{-1})	Assignment	Compounds
479	C1–O–C-4 glucoside bond [22]	Starch [23]
525	Skeletal vibration [24]	Fructose [23]
874	C–O–C cyclic alkyl ethers	Fructose [23,25]
876	Asymmetric stretching vibrations of the choline $N+(CH_3)_3$ group	Phospholipid [26]
942	C–O–C α-1-6 anomer	Starch [19,27,28]
952	C–O–C α-1-4 anomer	Starch [19,27]
1082	P═O stretching	Phytic acid [12]
1262	C-H stretching mode	Amide III structural proteins [29,30]
1265	Vibration of C-OH and C-OH [31]	Glucose / Fructose [25]
1320	Aliphatic side-chain stretching	Protein [32]
1374	HCC, HCO and HOC bending	β-Glucan [12]
1451–1455	HCH stretching	Gluten [12]

3.3. Different samples of Lanzhou lily

3.3.1. Picking time

Normally, farmers rely on experiences to determine when to harvest lily. But to ensure market supply, Lanzhou lilies can be harvested at any time except the coldest period in winter. We used Raman microscope to measure the samples of Lanzhou lily with different picking time, and compared the differences of nutrient components in these samples from the perspective of Raman spectrum.

Fig. 6 shows the contrast spectrum of two batches and there are significant differences between two spectra. Although the high intensity of starch Raman peak has obscured the peaks of other substances, in is notable that 874 cm^{-1} peak of the second batch shows much higher intensity, with little difference of typical starch peaks at 479 cm^{-1} and 942 cm^{-1}. The 525 cm^{-1}peak intensity of the second batch s is also much higher than that of the first batch, which demonstrates greater abundance of fructose and arabinose in such lilies. That is why Lanzhou lilies harvested at normal digging time show higher sweetness than at other times. The peak around 1380 cm^{-1} associated with HCC, HCO and HOC bending vibration are attributed to the contribution of β-glucan. It's a polysaccharide made up of glucose units, and most of them bind through β-1, 3, by which the glucose chain is connected. It can activate macrophages, neutrophils, monocytes, natural killer cells and dendritic cells [33], so it can increase leukin, cytokinin and specific antibody levels, and overall stimulate the body's immune system. This may reveal the health efficacy of the second batch. In addition, peaks at 1606 cm^{-1} and 1640 cm^{-1} used to be mentioned always occur in a consistent manner, which to some extent represent that the concentrations of amino acid and ferulic acid in this batch of samples are higher.

The noteworthy difference lies in the intensity ratio of the band 479 cm^{-1}, which is related to the vibration of pyranose skeletal and the band 942 cm^{-1}, which is related to the vibration of C–O–C α-1-6 anomer [19,27]. This reflects the differences in amylum structure between these two samples. It is concluded that, the major nutrient components can be qualitatively and quantitatively analyzed by Raman spectroscopy, and then the quality of lily bulbs can be evaluated.

Starch exists in the form of starch granules in advanced plants. The size and shape of starch granules vary with plant species and growing

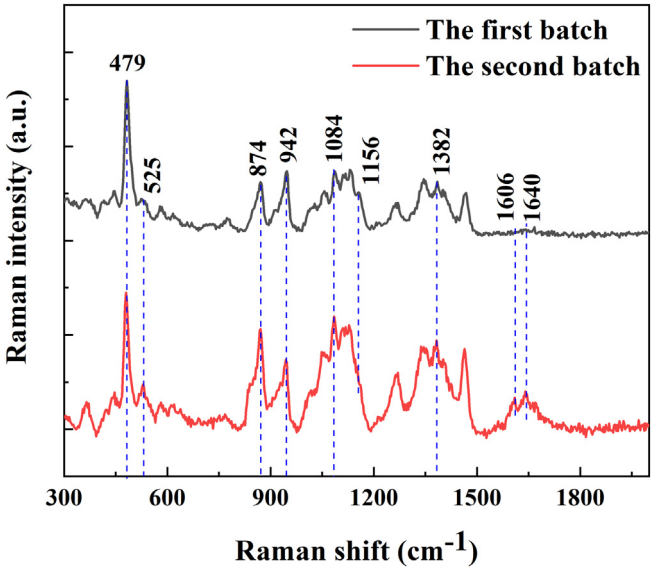

Fig. 6. Raman spectra of Lanzhou lilies after 15 days storage (Outer scales are used for comparison).

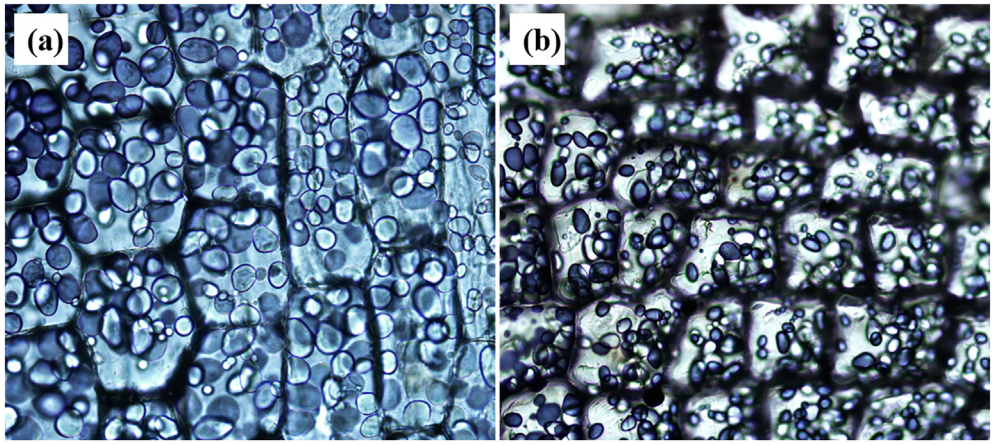

Fig. 7. Micrograph of I_2KI-stained lily bulb sections using (a) 200 × and (b) 100× microscopes.

place [2]. By I_2KI staining of lily sections in Fig. 7, we can see the homogeneous distribution of lily starch granules in cells. The starch granules of wheat, corn, potato, and rice starch have been studied extensively. Here, the starch granules in lily bulb samples are investigated by Raman spectroscopy. The imaging of lily bulb starch obtained by Raman microscope are shown in Fig. 8(a-b), which is consistent with the previous Xia Li's study using SEM [2]. They are always irregularly elliptic or cylindrical. Amylopectin intersections are linked by α (1 → 6) anomer glycoside bonds, which are much lower in amylose than in amylopectin. The band at 942 cm^{-1} is sensitive to the level of branching of the polysaccharide, band near the 1127 cm^{-1} is also relative to this chemical bond consequently. The enhancement of strength at 479 cm^{-1} was found to be positively correlated with the improvement of starch crystallinity [27,34].

Consider the Raman imaging at 479 cm^{-1} to be the distribution of starch, the integral image of 942 cm^{-1} to be a superimposed distribution of amylose and amylopectin. Then the details of amylopectin can be revealed by combining these two bands. The brightest spot in Fig. 8 (c-d) maps the crystalline region of amylose. The 1127 cm^{-1} peak is contributed by amylopectin. It has been reported that the ratio of amylose to amylopectin is related to the plant species, the growth temperature, climatic conditions and soil type [35,36]. In previous studies chemical methods were used to estimate the structural characteristics of starches extracted from common crops. This ratio of potato starch is lower than that of other cereal crops [37,38]. The Raman spectra indicate that this ratio of Lanzhou lily starch was even lower than potato starch (Fig. 5(a)), especially for those samples after a period of storage. This makes Lanzhou lily bulbs show more characteristics of amylopectin. Amylopectin is a highly branched molecule, which is the main reason for the crystallization of starch granules [39]. Vamadevan et al. [40] have drawn a conclusion that amylopectin starches possess low onset gelatinization temperatures and enthalpy values. As a result, amylopectin is easily digested and absorbed by the body. In other words, Lanzhou lily is friendly to the human digestive system.

Fig. 8(g- h) shows the distribution of proteins in the regions. Raman images suggest that starch granules scattered in a protein-filled matrix in cells are surrounded by proteins. In addition, the Raman images in Fig. 8(i-j) obtained by the integration of 874 cm^{-1} band show a directional characteristics, which is in connection with the birefringence [41] of starch granules. The vertical and horizontal directions of two regions have different intensity distributions. Placement direction of the samples during measurement determines the brightness characteristics in the center of the imaging region. This phenomenon is similar to the Maltese cross [42] starch under polarized light microscope, even if they are fundamentally different in origin [27]. The peaks related to starch polarization orientation mentioned in literature [27] are usually 860 cm^{-1} or 865 cm^{-1}, but in another study [20] this band is replaced by the band located at 873 cm^{-1}, here we believe that the peak at 874 cm^{-1} in this paper is equivalent to these peaks.

3.3.2. Size and weight

By current market standards, the large “one-headed” lilies are known as premium lilies and they are usually packaged separately. Similarly, the medium size is known as the “two-headed” or “three-headed”

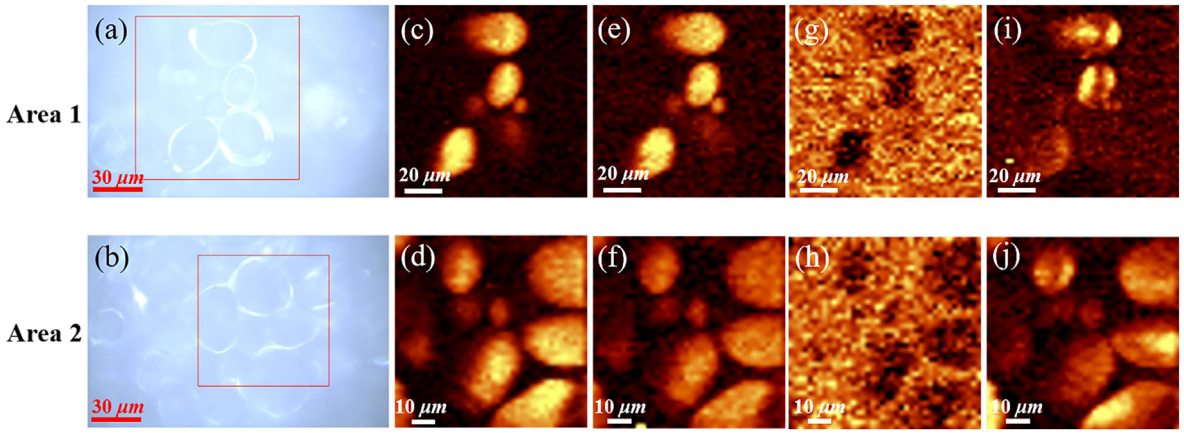

Fig. 8. Microscopic photograph (a, b) and Raman maps of two areas: (c, d) calculated from the Raman band at 479 cm^{-1}; (e, f) 942 cm^{-1}; (g, h) 1320 cm^{-1}; (i, j) 874 cm^{-1} The color scale is the same in (c-f) (The two areas in two photos were from the matrix of a typical sample of Lanzhou lily, with the size of 100 × 100 μm^2 and 80 × 80 μm^2 in the red box. Raman imaging was carried out on two regions respectively, 50 × 50 and 40 × 40 pixels were scanned).

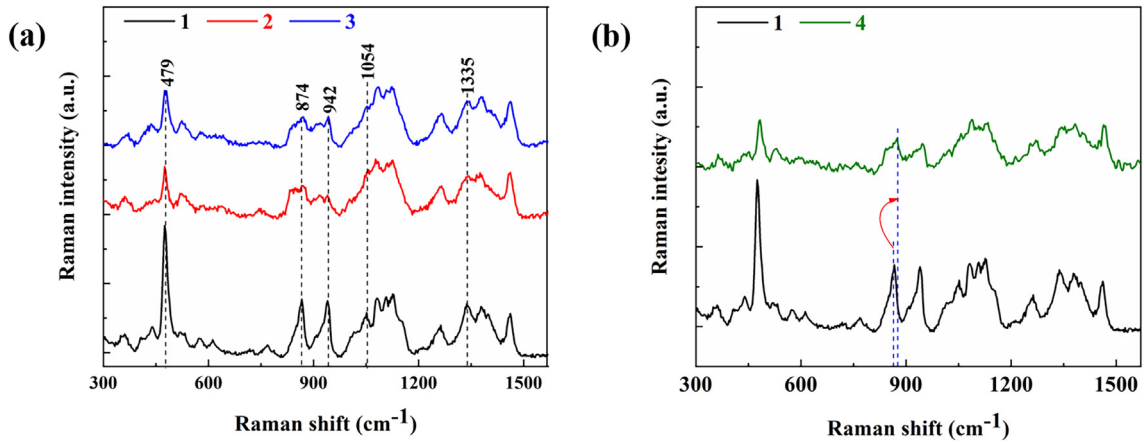

Fig. 9. Normalized Raman spectrum of Lanzhou lilies with: (a) different sizes; (b) split lily and round lily (Outer scales are used for comparison).

lilies, which earn the largest market share. We compared representative lily samples in different sizes and shapes, and Raman spectra of representative samples are given in Fig. 9.

Sample 1 is premium "one-headed" lily, with large diameter and a mass of more than 100 g. Sample 2 is of medium size, usually "double-headed" or even multi-headed. Sample 3 has the minimum size, which is usually used as a seed. The peaks in Raman spectrum of Sample 1 are much stronger, indicating that its carbohydrate storage is much more than that of two other samples. Very similar Raman spectra are observed for Samples 2 and 3, which indicates that there is no significant difference between the multi-head lilies and seeds in composition.

An important skeletal vibration is located near 479 cm^{-1}, which reflects a higher relative concentration of amylose in sample 1 than in smaller individuals. This illustrates large lily bulbs, as food, have a lower glycemic index [43] than inferior bulbs. At 874 cm^{-1} and 1054 cm^{-1}, corresponding to sucrose (or fructose) concentration, large Lanzhou lilies showed higher levels, confirming a positive correlation between diameter and sweetness. Likewise, the band at 1335 cm^{-1} is a vibration that originates from protein side chains [44], in where the larger lilies also perform better, proving that the larger bulb is richer in protein.

Another type of Lanzhou lily is common in the market. During their planting and development, the bulbs are divided into petals. Sample 4 is a slightly split bulb of Lanzhou lily and has almost the same mass and diameter as sample 1. Fig. 9(b) gives the Raman spectrum comparison of them. Apparently, spectrum of sample 4 is similar to that of the smaller sample in Fig. 9(a), and the carbohydrate's signature band is much less intense than that of sample 1, even though they are often intuitively considered to be similar in quality to the larger bulbs. This suggests that the split bulbs have lower levels of protein. It is notable that all bands on this spectrum have a small deviation from the positions of the well-shaped round lily samples. This conclusion implies that the bulb integrity affects the quality of Lanzhou lily essentially.

4. Conclusion

We creatively applied Raman spectrum and Raman imaging techniques for analysis of the components in Lanzhou lily bulb. The results prove that it is feasible to analyze major components in lily bulbs by Raman spectroscopy, which provide a nondestructive optical detection method for evaluation of lily quality. Samples of different locations, different sizes, different storage time and different harvest time showed significant changes in Raman spectra, indicating the change of nutrient contents. This offers an ideal method for Non-biochemical professionals to study the chemical compositions of lilies since the complex processing of chemical measurement for the preparation of samples is eliminated. However, Raman spectrum has its limitations: it is difficult to find evidence of high vitamin B2 (riboflavin) content and existence of some bioactive constituents in Lanzhou lily from Raman spectrum, and the unique medicinal value of Lanzhou lily cannot be fully reflected from Raman spectrum. In short, this method shows the potential of applying Raman spectroscopy and Raman imaging to agricultural science.

CRediT authorship contribution statement

Yuee Li: Conceptualization, Resources, Supervision, Writing - review & editing. **Huihui Wang:** Software, Investigation, Data curation, Writing - original draft. **Wenbo Zhang:** Visualization, Validation. **Haining Wu:** Software. **Zhong Wang:** Funding acquisition.

Declaration of competing interest

The authors declare that they have no known competing financial interests or personal relationships that could have appeared to influence the work reported in this paper.

Acknowledgment

This work was supported by the National Natural Science Foundation of China [grant number 61405083] and the Fundamental Research Funds for the Central Universities [grant numbers lzujbky-2018-129].

References

[1] Chinese flora Committee, C. A. o. S, Flora of China, 14, Science Press, Beijing, China, 1980.
[2] X. Li, W. Gao, Q. Jiang, Y. Xia, Physicochemical, morphological, and thermal properties of starches separated from bulbs of four Chinese lily cultivars, Starch - Stärke 64 (7) (2012) 545–551.
[3] E. Lee, N. Yun, Y.P. Jang, J. Kim, Lilium lancifolium Thunb. extract attenuates pulmonary inflammation and air space enlargement in a cigarette smoke-exposed mouse model, J. Ethnopharmacol. 149 (1) (2013) 148–156.
[4] D.T. Yang, Y.B. Ying, Applications of Raman spectroscopy in agricultural products and food analysis: a review, Appl. Spectrosc. Rev. 46 (7) (2011) 539–560.
[5] N. Altangerel, G.O. Ariunbold, C. Gorman, M.H. Alkahtani, E.J. Borrego, D. Bohlmeyer, P. Hemmer, M.V. Kolomiets, J.S. Yuan, M.O. Scully, In vivo diagnostics of early abiotic plant stress response via Raman spectroscopy, P. Natl. Acad. Sci. USA 114 (13) (2017) 3393–3396.
[6] A. Kudelski, Analytical applications of Raman spectroscopy, Talanta 76 (1) (2008) 1–8.
[7] M. Szymańska-Chargot, M. Chylińska, P.M. Pieczywek, P. Rösch, M. Schmitt, J. Popp, A. Zdunek, Raman imaging of changes in the polysaccharides distribution in the cell wall during apple fruit development and senescence, Planta 243 (4) (2016) 935–945.
[8] C. Krafft, C. Cervellati, C. Paetz, B. Schneider, J. Popp, Distribution of amygdalin in apricot (Prunus armeniaca) seeds studied by Raman microscopic imaging, Appl. Spectrosc. 66 (6) (2012) 644–649.
[9] D.W. Shipp, E.A. Rakha, A.A. Koloydenko, R.D. Macmillan, I.O. Ellis, I. Notingher, Intra-operative spectroscopic assessment of surgical margins during breast conserving surgery, Breast Cancer Res. 20 (1) (2018) 69.

[10] F. Tian, J. Conde, C. Bao, Y. Chen, J. Curtin, D. Cui, Gold nanostars for efficient in vitro and in vivo real-time SERS detection and drug delivery via plasmonic-tunable Raman/FTIR imaging, Biomaterials 106 (2016) 87–97.
[11] L. Zhu, J. Sun, G. Wu, Y. Wang, H. Zhang, L. Wang, H. Qian, X. Qi, Identification of rice varieties and determination of their geographical origin in China using Raman spectroscopy, J. Cereal Sci. 82 (2018) 175–182.
[12] A.-S. Jääskeläinen, U. Holopainen-Mantila, T. Tamminen, T. Vuorinen, Endosperm and aleurone cell structure in barley and wheat as studied by optical and Raman microscopy, J. Cereal Sci. 57 (3) (2013) 543–550.
[13] E. Graf, Antioxidant potential of ferulic acid, Free Radical Biology and Medicine 13 (4) (1992) 435–448.
[14] W. Tingting, Studies on Chemical Constituents of Lilium and Pyrus Cultivars, Tianjin University, 2015.
[15] J. De Gelder, K. De Gussem, P. Vandenabeele, L. Moens, Reference database of Raman spectra of biological molecules, J. Raman Spectrosc. 38 (9) (2007) 1133–1147.
[16] G.M. Symons, Y.-J. Chua, J.J. Ross, L.J. Quittenden, N.W. Davies, J.B. Reid, Hormonal changes during non-climacteric ripening in strawberry, J. Exp. Bot. 63 (13) (2012) 4741–4750.
[17] F. Denny, Hastening the sprouting of dormant potato tubers, Am. J. Bot. (1926) 118–125.
[18] W. Lihua, L. Jianlong, Physical and chemical properties of lily starch, Shandong Food Ferment 04 (1999) 51–56.
[19] S. Cael, J. Koenig, J. Blackwell, Infrared and Raman spectroscopy of carbohydrates: part III: Raman spectra of the polymorphic forms of amylose, Carbohydr. Res. 29 (1) (1973) 123–134.
[20] O. Piot, J.C. Autran, M. Manfait, Spatial distribution of protein and phenolic constituents in wheat grain as probed by confocal Raman microspectroscopy, J. Cereal Sci. 32 (1) (2000) 57–71.
[21] G. Wen-ling, L. Shi-feng, L. Ye-fang, C. Xian, L. Dong-hui, Analysis and assessment for nutrient contents in bulb of Cardiocrinum giganteum, Journal of West China Forestry Science 40 (01) (2011) 8–11.
[22] N.A. Nikonenko, D.K. Buslov, N.I. Sushko, R.G. Zhbankov, Investigation of stretching vibrations of glycosidic linkages in disaccharides and polysaccarides with use of IR spectra deconvolution, Biopolymers 57 (4) (2000) 257–262.
[23] E. Wiercigroch, E. Szafraniec, K. Czamara, M.Z. Pacia, K. Majzner, K. Kochan, A. Kaczor, M. Baranska, K. Malek, Raman and infrared spectroscopy of carbohydrates: a review, Spectrochim Acta A Mol Biomol Spectrosc 185 (2017) 317–335.
[24] M. Mathlouthi, D.V. Luu, Laser-Raman spectra of d-glucose and sucrose in aqueous solution, Carbohydr. Res. 81 (2) (1980) 203–212.
[25] A.N. Batsoulis, N.G. Siatis, A.C. Kimbaris, E.K. Alissandrakis, C.S. Pappas, P.A. Tarantilis, P.C. Harizanis, M.G. Polissiou, FT-Raman spectroscopic simultaneous determination of fructose and glucose in honey, J. Agric. Food Chem. 53 (2) (2005) 207–210.
[26] K. Czamara, K. Majzner, M.Z. Pacia, K. Kochan, A. Kaczor, M. Baranska, Raman spectroscopy of lipids: a review, J. Raman Spectrosc. 46 (1) (2015) 4–20.
[27] N. Wellner, D.M.R. Georget, M.L. Parker, V.J. Morris, In situ Raman microscopy of starch granule structures in wild type and ae mutant maize kernels, Starch - Stärke 63 (3) (2011) 128–138.
[28] Y. Liu, D.S. Himmelsbach, F.E. Barton, Two-dimensional Fourier transform Raman correlation spectroscopy determination of the glycosidic linkages in amylose and amylopectin, Appl. Spectrosc. 58 (6) (2004) 745–749.
[29] F. Bonnier, H.J.A. Byrne, Understanding the molecular information contained in principal component analysis of vibrational spectra of biological systems, Analyst 137 (2) (2012) 322–332.
[30] Y. Li, R. Shen, H. Wu, L. Yu, Z. Wang, D. Wang, Liver changes induced by cadmium poisoning distinguished by confocal Raman imaging, Spectrochim Acta A Mol Biomol Spectrosc 225 (2020) 117483.
[31] M.M. Paradkar, J. Irudayaraj, Discrimination and classification of beet and cane inverts in honey by FT-Raman spectroscopy, Food Chem. 76 (2) (2002) 231–239.
[32] A. Rygula, K. Majzner, K.M. Marzec, A. Kaczor, M. Pilarczyk, M. Baranska, Raman spectroscopy of proteins: a review, J. Raman Spectrosc. 44 (8) (2013) 1061–1076.
[33] C.F. Chan, W.K. Chan, D.M.-Y. Sze, The effects of β-glucan on human immune and cancer cells, J. Hematol. Oncol. 2 (1) (2009) 25.
[34] N. Dupuy, J. Laureyns, Recognition of starches by Raman spectroscopy, Carbohydr. Polym. 49 (1) (2002) 83–90.
[35] W.R. Morrison, T.P. Milligan, M.N. Azudin, A relationship between the amylose and lipid contents of starches from diploid cereals, J. Cereal Sci. 2 (4) (1984) 257–271.
[36] M. Asaoka, K. Okuno, H. Fuwa, Effect of environmental temperature at the milky stage on amylose content and fine structure of amylopectin of waxy and nonwaxy endosperm starches of rice (Oryza sativa L.), Agric. Biol. Chem. 49 (2) (1985) 373–379.
[37] H. Fredriksson, J. Silverio, R. Andersson, A.C. Eliasson, P. Åman, The influence of amylose and amylopectin on gelatinization and retrogradation properties of different starches, Carbohydr. Polymers 35 (3–4) (1998) 119–134.
[38] V. Vamadevan, E. Bertoft, Observations on the impact of amylopectin and amylose structure on the swelling of starch granules, Food Hydrocoll. 105663 (2020).
[39] A.J.F. Carvalho, 7 - Starch: major sources, properties and applications as thermoplastic materials, in: S. Ebnesajjad (Ed.), Handbook of Biopolymers and Biodegradable Plastics, William Andrew Publishing, Boston 2013, pp. 129–152.
[40] V. Vamadevan, E. Bertoft, K. Seetharaman, On the importance of organization of glucan chains on thermal properties of starch, Carbohydr. Polym. 92 (2) (2013) 1653–1659.
[41] H. Liu, J. Lelievre, W. Ayoungchee, A study of starch gelatinization using differential scanning calorimetry, X-ray, and birefringence measurements, Carbohydr. Res. 210 (1991) 79–87.
[42] L. Yang, Y. Xia, Y. Tao, H. Geng, Y. Ding, Y. Zhou, Multi-scale structural changes in lintnerized starches from three coloured potatoes, Carbohydr. Polym. 188 (2018) 228–235.
[43] D. Ludwig, The glycemic index, JAMA 287 (2002) 2414.
[44] L.Y. Zhou, Y. Yang, H.B. Ren, Y. Zhao, Z.J. Wang, F. Wu, Z.G. Xiao, Structural changes in rice bran protein upon different extrusion temperatures: a Raman spectroscopy study, Journal of Chemistry 2016 (2016) 1–8.